

Standing and traveling waves in Rayleigh-Bénard convection in cylindrical geometry

Katarzyna Boronska¹, Laurette S. Tuckerman²

Laboratoire d'Informatique pour la Mécanique et les Sciences de l'Ingénieur (LIMSI-CNRS)
B.P. 133, 91403 Orsay, France

¹e-mail: kasia@limsi.fr - Web page: <http://www.limsi.fr/Individu/kasia/>

²e-mail: laurette@limsi.fr - Web page: <http://www.limsi.fr/Individu/laurette/>

ABSTRACT

Even though the study of Rayleigh-Bénard convection has lasted nearly a century, the variety of patterns and dynamical behavior that it can display continues to astonish researchers [1,2]. One example is convection in a cylindrical container, which can take the form of concentric rolls or else a non-axisymmetric form as the temperature difference, measured by the Rayleigh number Ra is increased. The linear analysis of the pattern at threshold was carried out 20 years ago by Buell & Catton [3] for a range of values of the aspect ratio $\Gamma \equiv \text{radius/height}$. The secondary flows have been studied during the last 10 years, e.g. by Wanschura et al. [4], Touihri et al. [5], and Hof et al. [6] for several parameter combinations of Γ and the Prandtl number Pr .

Wanschura *et al.* [4] determined numerically that for $\Gamma = 1.47$, $Pr = 1$, the axisymmetric convective flow that was first produced upon increasing the Rayleigh number lost stability via a secondary Hopf bifurcation to eigenvectors with azimuthal wavenumber $m = 3$. A Hopf bifurcation in the presence of $O(2)$ symmetry, that is in a circle or cylinder in which no phase or direction is preferred, leads to competition between standing and traveling waves. Our goal has been to study the nonlinear patterns produced by the Hopf bifurcation.

The system is governed by the Navier-Stokes and Boussinesq equations:

$$\frac{\partial \mathbf{u}}{\partial t} + (\mathbf{u} \cdot \nabla) \mathbf{u} = -\nabla p + Pr \Delta \mathbf{u} + Ra Pr h \mathbf{e}_z \quad (1)$$

$$\frac{\partial h}{\partial t} + \mathbf{u} \cdot \nabla h = u_z + \Delta h \quad (2)$$

$$\nabla \cdot \mathbf{u} = 0 \quad (3)$$

where \mathbf{u} is the velocity field and h is the difference between the temperature field and the conductive solution. The boundary conditions are:

$$\mathbf{u} = 0 \quad \text{at } r = \Gamma \quad \text{and at } z = \pm 1/2 \quad (4)$$

$$h = 0 \quad \text{at } z = \pm 1/2 \quad (5)$$

$$\frac{\partial h}{\partial r} = 0 \quad \text{at } r = \Gamma \quad (6)$$

The fields \mathbf{u} and h are represented using Chebyshev polynomials in r and in z and Fourier series in θ :

$$f(r, z, \theta, t) = \sum_{j,k,m} \hat{f}_{jkm}(t) C_j(r/\Gamma) C_k(2z) e^{im\theta} + \text{c.c.} \quad (7)$$

The equations are integrated by a classical pseudospectral method, in which the nonlinear terms are calculated in physical space and integrated via the Adams-Bashforth formula, while the linear terms are calculated in spectral space and integrated via the Crank-Nicolson formula. The number of grid

points or modes used is $N_r = 36$, $N_\theta = 80$, $N_z = 18$. An influence matrix method is used to impose incompressibility [7].

For $\Gamma = 1.47$ and $Pr = 1$, the conductive solution undergoes a bifurcation towards steady convection in the form of axisymmetric rolls at $Ra = 1900$. Then, at $Ra \approx 25000$, this convective state undergoes in turn a Hopf bifurcation; the corresponding eigenvectors have azimuthal wavenumber $m = 3$.

At the linear stage, the temporal evolution of the $m = 3$ mode is described by

$$a_+ f_+(r, z) e^{im\theta - \omega t} + a_- f_-(r, z) e^{im\theta + \omega t} + a_+^* f_+^*(r, z) e^{-im\theta + \omega t} + a_-^* f_-^*(r, z) e^{-im\theta - \omega t} \quad (8)$$

where \mp indicates rotation in a clockwise or counter-clockwise direction, f_\pm are two complex eigenvectors, and a_\pm describes their amplitudes and phases, which are arbitrary at the linear stage, giving an evolution in a four-dimensional space.

The addition of nonlinear terms restricts the number of solutions to three:

$$f_+ \sim f_+(r, z) e^{im\theta - \omega t} + f_+^*(r, z) e^{-im\theta + \omega t} \quad (9)$$

$$f_- \sim f_-(r, z) e^{im\theta + \omega t} + f_-^*(r, z) e^{-im\theta - \omega t} \quad (10)$$

$$f_s \sim f_+ + f_- \quad (11)$$

These are counter-clockwise traveling waves f_+ , clockwise traveling waves f_- , and standing waves f_s which are an exact superposition of the two traveling wave solutions. Of these possible solutions, either standing waves are stable (figure 1, left), or the traveling wave solutions are stable (figure 1, right), or none are stable [8,9].

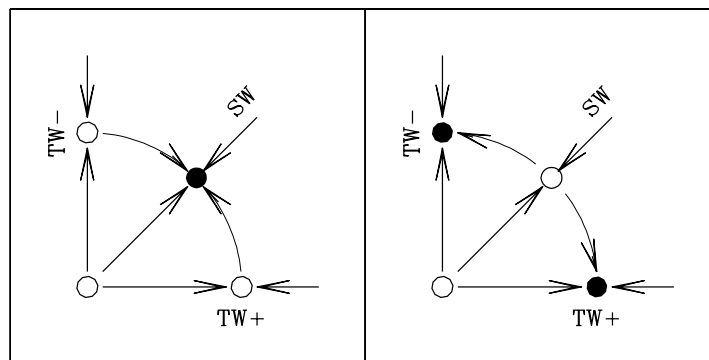


Figure 1: Phase diagram illustrating stability of standing waves (left) or of traveling waves (right).

We observe, first, standing waves, illustrated by figures 2 and 3. After a sufficiently long integration time has elapsed, the standing waves are replaced by traveling waves, illustrated by 4 and 5. All of the states have an azimuthal spatial period of $2\pi/3$. In addition, the standing waves have six axes reflection symmetry, while this symmetry is broken for the traveling waves.

The explanation of this behavior is that the standing waves are stable when reflection symmetry is imposed and weakly unstable otherwise. Since the initial conditions are reflection symmetric, the flow evolves rapidly towards standing waves, and then slowly towards the traveling waves, which are stable.

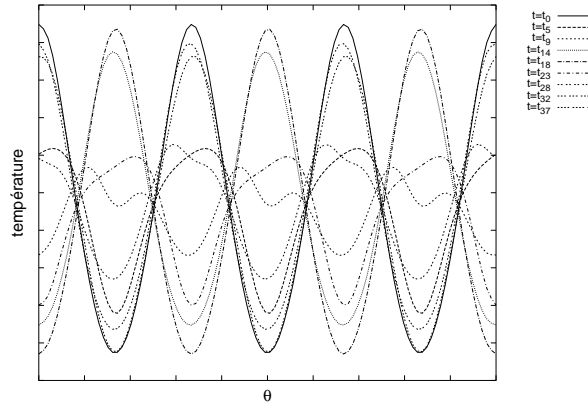


Figure 2: Standing waves: temperature as a function of angle for fixed height and radius at different instants in time.

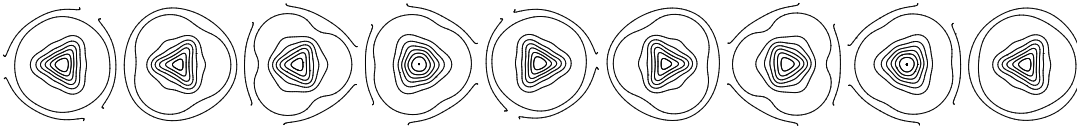


Figure 3: Evolution of the temperature during a period of standing waves.

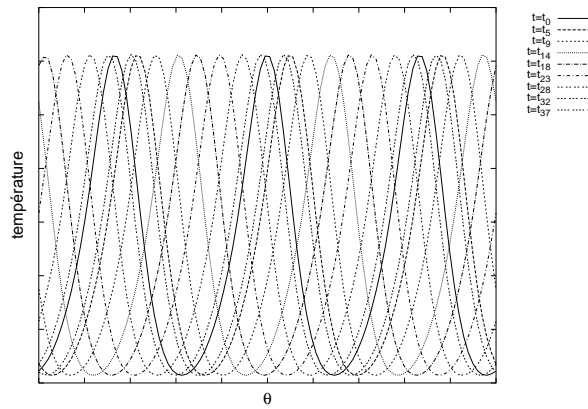


Figure 4: Traveling waves: temperature as a function of angle.



Figure 5: Evolution of the temperature field during the traveling waves.

REFERENCES

- [1] V. Croquette, *Convective pattern dynamics at low Prandtl number*, Contemporary Physics, Part I: **30**, 113 ; Part II: **30**, 153 (1989).
- [2] E. Bodenschatz, W. Pesch & G. Ahlers, *Recent Developments in Rayleigh-Bénard Convection*, Annu. Rev. Fluid Mech. **32**, 709 (2000).
- [3] J.C. Buell & I. Catton, *The effect of wall conduction on the stability of a fluid in a right circular cylinder heated from below*, Journal of Heat Transfer **105**, 255 (1983).
- [4] M. Wanschura, H.C. Kuhlmann & H.J. Rath, *Three-dimensional instability of axisymmetric buoyant convection in cylinders heated from below*, J. Fluid Mech. **326**, 399 (1996).
- [5] R. Touihri, H. BenHadid & D. Henry, *On the onset of convective instabilities in cylindrical cavities heated from below. I. Pure thermal case*, Phys. Fluids **11**, 2078 (1999).
- [6] B. Hof, P.G.J. Lucas & T. Mullin, *Flow state multiplicity in convection*, Phys. Fluids **11**, 2815 (1999).
- [7] L.S. Tuckerman, *Divergence-free velocity fields in nonperiodic geometries*, J. Comput. Phys. **80**, 403 (1989).
- [8] M. Golubitsky & I. Stewart, *Hopf bifurcation in the presence of symmetry*, Arch. Rat. Mech. **87**, 107 (1985).
- [9] E. Knobloch, A.E. Deane, J. Toomre & D.R. Moore, *Doubly diffusive waves*, Contemporary Math. **56**, 203 (1986).